

# Two-Phase and Vapor Phase $PvTx$ Properties of the Difluoromethane + *cis*-1,3,3,3-Tetrafluoroprop-1-ene Binary System

Sebastiano Tomassetti, Giovanni Di Nicola,\* Mariano Pierantozzi, and J. Steven Brown

Cite This: *J. Chem. Eng. Data* 2020, 65, 4326–4334

Read Online

ACCESS |



Metrics &amp; More

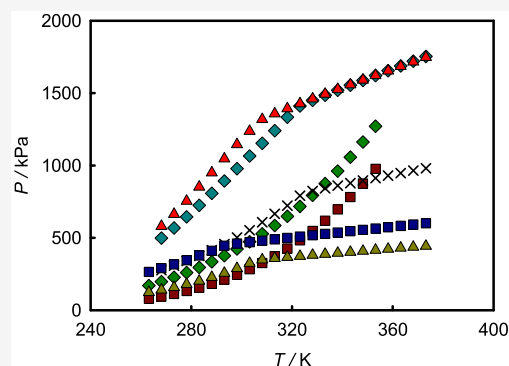


Article Recommendations



Supporting Information

**ABSTRACT:** This paper provides 84 two-phase and 66 vapor phase  $PvTx$  measurements for binary blends comprising difluoromethane (R32) and *cis*-1,3,3,3-tetrafluoroprop-1-ene (R1234ze(Z)). The data are for seven isochores (0.013352, 0.016365, 0.023746, 0.026769, 0.035001, 0.070089, 0.071713)  $\text{m}^3 \cdot \text{kg}^{-1}$  for the temperature range from (263 to 373) K for seven R32 mole fractions (0.0871, 0.2980, 0.3620, 0.5232, 0.7128, 0.8015, 0.8973). The flash method coupled with the Peng–Robinson equation of state and a two-parameter cubic equation of state proposed by Stryjek was used to derive the vapor–liquid equilibrium of the R32 (1) + R1234ze(Z) (2) binary pair from the two-phase measurements. The measured properties in the superheated vapor region were correlated through the aforementioned equations of state and a truncated virial equation of state. The  $PvTx$  data display good agreement with both the values calculated from the equations of state and from REFPROP 10.0 predictions.



## INTRODUCTION

Many hydrofluorocarbon (HFC) refrigerants are potent greenhouse gases with increasingly stringent restrictions being placed on their productions and uses.<sup>1,2</sup> As a result, the heating, ventilating, air conditioning, and refrigeration (HVAC&R) industry is increasingly being forced to actively seek low global warming potential (GWP) alternatives to more conventional HFC working fluids.

McLinden et al.<sup>3,4</sup> recently conducted exhaustive searches and analyses of a publicly available database containing more than 60 million chemical substances for possible applications as low GWP working fluids in HVAC&R applications. They showed that only a small number of single-component working fluids possess the right combination of environmental (e.g., low GWP and essentially no ozone depletion potential), safety (e.g., flammability and toxicity), and performance (e.g., energy efficiency and appropriate volumetric cooling (or heating) capacity) characteristics for many HVAC&R applications. All is not lost, however, as one way to overcome this limited pool of single-component options is to blend them in order to optimize the desired characteristics of the blended working fluid for the application of interest.

The authors have previously reported vapor phase  $PvTx$  data for 12 binary blends of low GWP refrigerants: (1) nitrogen + *trans*-1,3,3,3-tetrafluoroprop-1-ene,<sup>5</sup> (2) methane + *trans*-1,3,3,3-tetrafluoroprop-1-ene,<sup>5</sup> (3) propane + 2,3,3,3-tetrafluoroprop-1-ene,<sup>6</sup> (4) propane + *cis*-1,2,3,3,3-pentafluoroprop-1-ene,<sup>6</sup> (5) isobutane + 2,3,3,3-tetrafluoroprop-1-ene,<sup>7</sup> (6) isobutane + *trans*-1,3,3,3-tetrafluoroprop-1-ene,<sup>7</sup> (7) isobutane + *cis*-1,3,3,3-tetrafluoroprop-1-ene,<sup>8</sup> (8) isobutane + *trans*-1-chloro-3,3,3-trifluoroprop-1-ene,<sup>8</sup> (9) isobutane + *cis*-

1,2,3,3,3-pentafluoroprop-1-ene,<sup>9</sup> (10) isobutane + 3,3,3-trifluoropropene,<sup>9</sup> (11) difluoromethane + 2,2,2,3-tetrafluoroprop-1-ene,<sup>10</sup> and (12) difluoromethane + *trans*-1,3,3,3-tetrafluoroprop-1-ene.<sup>11</sup>

The present paper expands the authors' work by presenting 150  $PvTx$  measurements for binary blends consisting of difluoromethane (R32) and *cis*-1,3,3,3-tetrafluoroprop-1-ene (R1234ze(Z)) both in the two-phase and superheated vapor regions using an isochoric test cell. The measured data are correlated with several equations of state, as well as are compared with REFPROP 10.0<sup>12</sup> predictions. The combination of the experimental data and the accompanying fitting models presented herein expand the publicly available thermodynamic property database of low-GWP refrigerant blends.

## EXPERIMENTAL SECTION

**Materials.** Table 1 provides details for the samples of difluoromethane (R32,  $\text{CH}_2\text{F}_2$ , CASRN 75-10-5) and *cis*-1,3,3,3-tetrafluoroprop-1-ene (R1234ze(Z),  $\text{CF}_3\text{CH}=\text{CHF}$ , CASRN 29118-25-0). The measured samples were subjected to several cycles of freezing, evacuation, thawing, and ultrasonic stirring to remove any remaining noncondensable

Special Issue: Alternative Refrigerants

Received: April 13, 2020

Accepted: June 24, 2020

Published: July 6, 2020



Table 1. Descriptions of R32 and R1234ze(Z) Samples

chemical name	CASRN	source	initial mole fraction purity	purification method	final mole fraction purity	analysis method
R32 <sup>a</sup>	75-10-5	Ausimont SpA	0.9957	several cycles of freezing, evacuation, melting, and ultrasonic agitation	0.9998	GC
R1234ze(Z) <sup>b</sup>	29118-25-0	Central Glass Ltd.	>0.99 <sup>c</sup>	several cycles of freezing, evacuation, melting, and ultrasonic agitation	0.9970	GC

<sup>a</sup>Difluoromethane. <sup>b</sup>*cis*-1,3,3,3-Tetrafluoroprop-1-ene. <sup>c</sup>Value reported in the manufacturer's data sheet.

Table 2. Bulk Mole Fractions  $z$ , Average Specific Volumes  $\nu$ , Temperature Ranges  $\Delta T$ , Pressure Ranges  $\Delta P$ , Numbers of Charged Moles  $n$ , and Amounts of Charged Masses  $m$  for Binary Blends of R32 (1) and R1234ze(Z) (2)

series	$z_1$	$\nu/\text{m}^3\cdot\text{kg}^{-1}$	$\Delta T/\text{K}$	$\Delta P/\text{kPa}$	$n/\text{mol}$	$m_1/\text{g}$	$m_2/\text{g}$
1	0.0871	0.013352	263.15–353.15	79.5–976.6	0.1887	0.855	19.649
2	0.2980	0.016365	263.15–353.15	170.4–1270.8	0.1751	2.714	14.016
3	0.3620	0.071713	263.15–373.15	123.8–443.2	0.0417	0.785	3.034
4	0.5232	0.035001	268.15–373.15	276.8–981.0	0.0959	2.610	5.214
5	0.7128	0.070089	263.15–373.15	264.9–600.6	0.0560	2.075	1.833
6	0.8015	0.023746	268.15–373.15	498.2–1752.9	0.1793	7.477	4.059
7	0.8973	0.026769	268.15–373.15	579.9–1747.3	0.1753	8.181	2.052

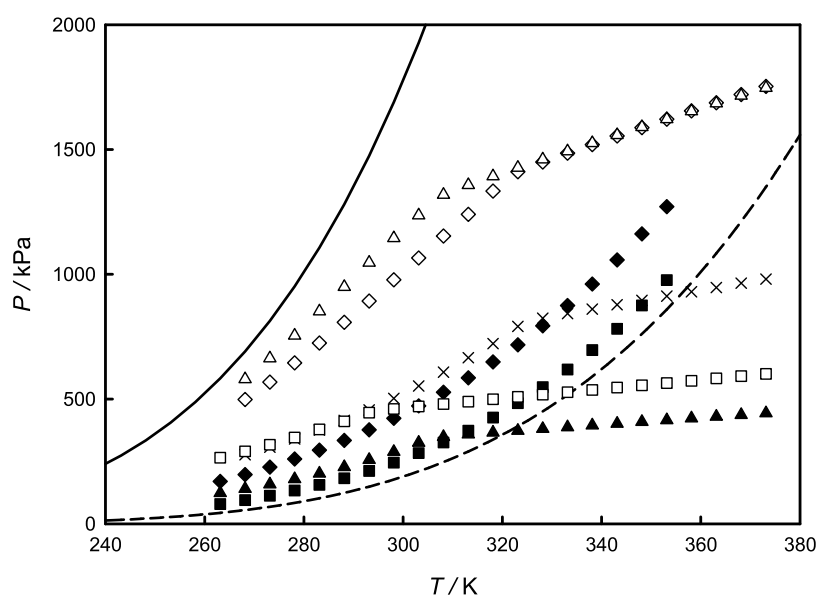


**Figure 1.** Pressure  $P$ , temperature  $T$ , bulk mole fraction  $z$ , and specific volume  $\nu$  data (Table 3 and Table SI in the Supporting Information) for R32 (1) + R1234ze(Z) (2) binary blends measured both in the two-phase and superheated vapor regions:  $\blacksquare$ ,  $z_1 = 0.0871$  and  $\nu = 0.013352 \text{ m}^3\cdot\text{kg}^{-1}$ ;  $\blacklozenge$ ,  $z_1 = 0.2980$  and  $\nu = 0.016365 \text{ m}^3\cdot\text{kg}^{-1}$ ;  $\blacktriangle$ ,  $z_1 = 0.3620$  and  $\nu = 0.071713 \text{ m}^3\cdot\text{kg}^{-1}$ ;  $\times$ ,  $z_1 = 0.5232$  and  $\nu = 0.035001 \text{ m}^3\cdot\text{kg}^{-1}$ ;  $\square$ ,  $z_1 = 0.7128$  and  $\nu = 0.070089 \text{ m}^3\cdot\text{kg}^{-1}$ ;  $\diamond$ ,  $z_1 = 0.8015$  and  $\nu = 0.023746 \text{ m}^3\cdot\text{kg}^{-1}$ ;  $\triangle$ ,  $z_1 = 0.8973$  and  $\nu = 0.026769 \text{ m}^3\cdot\text{kg}^{-1}$ . The behaviors of the vapor pressure for R32 (solid line) and R1234ze(Z) (dashed line) calculated by REFPROP 10.0 are also shown.

gases. A gas chromatograph (GC) with a thermal conductivity detector was used to verify the R32 purity. The mole fraction purities measured with the GC and reported in Table 1 are the GC peak area percentages.

**Experimental Apparatus and Procedure.** The experimental apparatus consists of an isochoric sphere and two separate thermostatic baths capable of operating in a lower temperature range of (210 to 298) K and in a higher temperature range of (303 to 390) K. Only a summary description of the experimental setup and test procedures are provided below since more detailed descriptions are provided elsewhere.<sup>7,8,13,14</sup>

A gravimetric method was used to prepare the binary blends. To begin, the desired mass of the lower pressure refrigerant (refrigerant 1) was discharged into an evacuated container (container 1), of known tare weight, and weighed using an

analytical balance possessing an uncertainty of  $\pm 0.3$  mg. Next container 1 and a second evacuated container (container 2), of known tare weight, were both connected to the isochoric cell. The isochoric cell and all tubing were evacuated prior to connection. Next the desired mass of refrigerant 1 was discharged into the isochoric cell. After charging and isolating the isochoric cell, any refrigerant remaining in the connection tubing was recovered into container 2, after which the masses of both containers 1 and 2 were measured. The mass of refrigerant 1 charged into the isochoric cell was determined to be the difference in the combined masses of containers 1 and 2 before and after charging of refrigerant 1 into the isochoric cell. The procedure was then repeated for the higher pressure refrigerant (refrigerant 2). The expanded uncertainty of the mass of the binary blend (refrigerant 1 + refrigerant 2) charged

**Table 3. Experimental Values of Temperature  $T$ , Pressure  $P$ , Specific Volume  $\nu$ , and Bulk Mole Fraction  $z$  in the Superheated Vapor Region for R32 (1) + R1234ze(Z) (2) Binary Blends<sup>a</sup>**

$T/K$	$P/kPa$	$\nu/m^3 \cdot kg^{-1}$	$T/K$	$P/kPa$	$\nu/m^3 \cdot kg^{-1}$
	$z_1 = 0.3620(16)$			$z_1 = 0.8015(3)$	
308.15 <sup>b</sup>	348.4 <sup>b</sup>	0.071682(79) <sup>b</sup>	323.15 <sup>b</sup>	1411.0 <sup>b</sup>	0.023749(26) <sup>b</sup>
313.15 <sup>b</sup>	358.7 <sup>b</sup>	0.071697(79) <sup>b</sup>	328.15	1450.1	0.023754(26)
318.15 <sup>b</sup>	366.4 <sup>b</sup>	0.071713(79) <sup>b</sup>	333.15	1485.3	0.023759(26)
323.15 <sup>b</sup>	373.6 <sup>b</sup>	0.071729(79) <sup>b</sup>	338.15	1519.9	0.023765(26)
328.15	380.7	0.071744(79)	343.15	1554.1	0.023770(26)
333.15	387.8	0.071760(79)	348.15	1587.9	0.023775(26)
338.15	394.8	0.071776(79)	353.15	1621.4	0.023780(26)
343.15	401.7	0.071792(79)	358.15	1654.6	0.023785(26)
348.15	408.8	0.071807(79)	363.15	1687.8	0.023791(26)
353.15	415.9	0.071823(79)	368.15	1720.5	0.023796(26)
358.15	422.9	0.071839(79)	373.15	1752.9	0.023801(26)
363.15	429.8	0.071854(79)			
368.15	436.5	0.071870(79)			
373.15	443.2	0.071886(79)			
	$z_1 = 0.5232(5)$			$z_1 = 0.8973(6)$	
323.15 <sup>b</sup>	791.3 <sup>b</sup>	0.035005(38) <sup>b</sup>	308.15 <sup>b</sup>	1318.8 <sup>b</sup>	0.026755(29) <sup>b</sup>
328.15	823.9	0.035012(38)	313.15 <sup>b</sup>	1358.1 <sup>b</sup>	0.026761(29) <sup>b</sup>
333.15	842.5	0.035020(38)	318.15 <sup>b</sup>	1393.0 <sup>b</sup>	0.026766(29) <sup>b</sup>
338.15	860.4	0.035028(38)	323.15	1427.2	0.026772(29)
343.15	878.1	0.035035(38)	328.15	1460.5	0.026778(29)
348.15	895.6	0.035043(38)	333.15	1493.5	0.026784(29)
353.15	912.6	0.035051(38)	338.15	1526.1	0.026790(29)
358.15	930.1	0.035058(38)	343.15	1558.4	0.026796(29)
363.15	947.2	0.035066(38)	348.15	1590.4	0.026802(29)
368.15	964.3	0.035074(38)	353.15	1622.2	0.026807(29)
373.15	981.0	0.035081(38)	358.15	1653.8	0.026813(29)
			363.15	1685.1	0.026819(29)
			368.15	1716.3	0.026825(29)
			373.15	1747.3	0.026831(29)
	$z_1 = 0.7128(9)$				
298.15 <sup>b</sup>	460.5 <sup>b</sup>	0.070027(77) <sup>b</sup>			
303.15	470.5	0.070043(77)			
308.15	480.3	0.070058(77)			
313.15	489.8	0.070074(77)			
318.15	499.3	0.070089(77)			
323.15	508.8	0.070104(77)			
328.15	518.2	0.070120(77)			
333.15	527.5	0.070135(77)			
338.15	536.8	0.070150(77)			
343.15	546.0	0.070166(77)			
348.15	555.2	0.070181(77)			
353.15	564.4	0.070196(77)			
358.15	573.5	0.070212(77)			
363.15	582.6	0.070227(77)			
368.15	591.7	0.070243(77)			
373.15	600.6	0.070258(77)			

<sup>a</sup>Expanded uncertainties are  $U(T) = 0.03$  K and  $U(P) = 1$  kPa.  $U(\nu)$  and  $U(z_1)$  at the 95% confidence level are provided between parentheses (the uncertainty values refer to the corresponding last digits of the experimental values). <sup>b</sup>Not included in the regression analysis.

into the isochoric cell with a coverage factor of 2 (95% confidence level) was determined to be 1.2 mg.

The temperatures of the thermostatic baths were measured using a Hart Scientific S680 platinum resistance (25 ohm) thermometer. The refrigerant pressure in the isochoric cell was measured using a Ruska 7000 pressure transducer. The volume ( $V_{\text{iso}}$ ) of the isochoric cell at 298 K was determined to be 273.3 cm<sup>3</sup>. As described elsewhere,<sup>13</sup> a correction for the thermal expansion of the isochoric cell was included. The expanded

uncertainties for the temperature, pressure, and volume with coverage factors of 2 (95% confidence level) were determined to be 0.03 K, 1 kPa, and 0.3 cm<sup>3</sup>, respectively. The expanded uncertainty of the pressure measurements included effects from changes in the thermostatic bath temperatures.

The uncertainties for the specific volumes and the mole fractions of the studied blends were estimated as reported elsewhere.<sup>7,8</sup> The uncertainty of the specific volume is a function of the uncertainties of the volume estimation and

**Table 4.** Absolute Average Relative Deviations of the Pressure (AARD ( $P$ )) Calculated by the “Flash Method” Coupled with the Select EoSs Using (a) Average  $\bar{k}_{12}$  Regressed from All the Two-Phase Measurements of the R32 (1) + R1234ze(Z) (2) Binary Blend and (b)  $k_{12}$  Adjusted for Each Isochore

series	$z_1$	PR EoS			Stryjek EoS			REFPROP 10.0
		AARD ( $P$ ) <sup>a</sup> /%	$k_{12}$	AARD ( $P$ ) <sup>b</sup> /%	AARD ( $P$ ) <sup>c</sup> /%	$k_{12}$	AARD ( $P$ ) <sup>b</sup> /%	AARD ( $P$ ) <sup>c</sup> /%
1	0.0871	0.48	0.00297	0.46	0.45	0.00012	0.41	7.66
2	0.2980	1.55	0.01258	0.34	1.65	0.00920	0.19	9.29
3	0.3620	0.79	-0.00637	0.25	0.86	-0.01045	0.33	6.46
4	0.5232	1.47	0.01366	0.56	1.55	0.01043	0.57	6.61
5	0.7128	0.58	-0.00272	0.33	0.61	-0.00577	0.38	6.08
6	0.8015	1.13	-0.00590	0.30	1.10	-0.00882	0.41	6.22
7	0.8973	1.19	-0.00849	0.35	1.18	-0.01140	0.37	4.29
avg		1.05		0.38	1.09		0.37	7.12

<sup>a</sup>Calculated using  $\bar{k}_{12} = 0.00281$ . <sup>b</sup>Calculated using  $k_{12}$  fitted for each series. <sup>c</sup>Calculated using  $\bar{k}_{12} = -0.00037$ .

mass measurements. On the basis of the propagation of uncertainty, the uncertainty of the mole fraction depends on the mass of the charged sample, the calculated specific volume, and the mole fraction itself. The expanded uncertainties in the specific volumes with coverage factors of 2 (95% confidence level) for the various blends are provided in Table SI in the Supporting Information and in Table 3. The expanded uncertainties with coverage factors of 2 (95% confidence level) for the various R32 mole fractions ( $z_1$ ) of binary blends of R32 (1) + R1234ze(Z) (2) are also provided in Table SI in the Supporting Information and in Table 3.

The measurement procedure consisted of allowing the thermostatic bath temperature to stabilize at the desired test temperature, after which a circulating pump within the isochoric cell mixed the refrigerant sample for 15 min. The refrigerant sample was then allowed to stabilize for an hour, after which the sample pressure was measured. The procedure was then repeated for all of the desired temperature levels.

## RESULTS AND DISCUSSION

In this section, the  $PvTx$  data for R32 (1) + R1234ze(Z) (2) binary system measured with the isochoric apparatus are reported. Moreover, the results obtained by comparing the experimental data with the values calculated using different models are presented.

**Experimental Data.**  $PvTx$  measurements for seven R32 (1) and R1234ze(Z) (2) blends were taken along isochores of (0.013352, 0.016365, 0.023746, 0.026769, 0.035001, 0.070089, 0.071713)  $\text{m}^3\cdot\text{kg}^{-1}$  for R32 mole fractions of (0.0871, 0.2980, 0.3620, 0.5232, 0.7128, 0.8015, 0.8973) over a temperature range from (263 to 373) K. Table 2 provides the measured temperature and pressure ranges for the seven blends, and in addition, the compositions, the average specific volumes, and the number of moles and masses charged into the isochoric cell, all for the same seven blends. Figure 1 shows  $P$ - $T$  behaviors for the seven isochores both in the two-phase and superheated vapor regions together with the behaviors of the vapor pressure for R32 and R1234ze(Z) calculated by REFPROP 10.0.<sup>12</sup> The demarcation points marking the boundaries between the two-phase and superheated vapor regions were determined from the changes in the slopes of the respective  $P$ - $T$  curves. The measured  $P$ - $T$  values for the two-phase region are reported in Table SI in the Supporting Information. Table 3 provides the measured  $P$ - $T$  values for the superheated vapor region.

**Vapor-Liquid Equilibrium Assessment.** The vapor-liquid equilibrium (VLE) properties of R32 (1) + R1234ze(Z)

(2) binary blends were determined from the two-phase  $PvTx$  measurements by implementing the “flash method” and (1) the Peng-Robinson Equation of State (PR EoS)<sup>15</sup> coupled with the van der Waals one-fluid mixing rules<sup>16</sup> with a binary interaction parameter ( $k_{12}$ ) and (2) a two-parameter cubic EoS proposed by Stryjek<sup>17,18</sup> coupled with the van der Waals one-fluid mixing rules<sup>16</sup> with a  $k_{12}$ . The latter EoS was chosen since it generally shows somewhat better VLE behavior for blends containing low-GWP refrigerants when compared with other, more conventional two-parameter cubic EoSs.<sup>19,20</sup>

As described elsewhere,<sup>10,21</sup> the “flash method” yields the values of  $P$  and of the mole fractions of the liquid phase ( $x_i$ ) and of the vapor phase ( $y_i$ ) for each isochoric point subject to isofugacity conditions and through the minimization of the difference between the calculated isochoric sphere volume and the experimental isochoric sphere volume estimated from the gravimetric calibration. While  $T$ ,  $z_i$ , and  $n$  are fixed at their experimental values for calculation purposes, the  $k_{12}$  values were determined by minimizing the following objective function:

$$Q = \sum_{i=1}^N \left( \frac{P_{\text{exp},i} - P_{\text{calc},i}}{P_{\text{exp},i}} \right)^2 \quad (1)$$

where  $N$  is the number of experimental data. The volume condition of the “flash” method requires the calculated (from the EoS) volumetric properties of the liquid and vapor phases.

Table 4 provides the absolute average relative deviations of the pressure (AARD ( $P$ )) provided by the “flash method” coupled with the PR<sup>15</sup> and the cubic EoS of Stryjek<sup>17,18</sup> using (a) average  $\bar{k}_{12}$  regressed from all the two-phase measurements of the R32 (1) + R1234ze(Z) (2) binary blend and (b)  $k_{12}$  adjusted for each isochore. The AARD ( $P$ ) was calculated from

$$\text{AARD}(P)/\% = \frac{100}{N} \sum_{i=1}^N \left| \frac{P_{\text{exp},i} - P_{\text{calc},i}}{P_{\text{exp},i}} \right| \quad (2)$$

Table 4 provides the  $\bar{k}_{12}$  values and the  $k_{12}$  values for each refrigerant blend. Table 5 provides pressures and compositions of liquid and vapor phases derived from the “flash method” with the select EoSs using the  $k_{12}$  values determined for each isochore. Figure 2 shows the relative deviations between the measured pressures and the values calculated with each EoS with the  $k_{12}$  values having been determined for each refrigerant blend. The resulting deviations are generally within  $\pm 1\%$  for nearly all of the experimental points.

**Table 5. Pressures  $P_{\text{calc}}$ , Mole Fractions of the Liquid Phase  $x_{1,\text{calc}}$ , and Mole Fractions of the Vapor Phase  $y_{1,\text{calc}}$  Estimated through the “Flash Method” Coupled with the Select EoSs Using  $k_{12}$  Adjusted for Each Bulk Mole Fraction  $z_1$  of the R32 (1) + R1234ze(Z) (2) Binary Blend (Table 4) for the Experimental Temperatures  $T$**

T/K	PR EoS			Stryjek EoS			T/K	PR EoS			Stryjek EoS		
	$P_{\text{calc}}/\text{kPa}$	$x_{1,\text{calc}}$	$y_{1,\text{calc}}$	$P_{\text{calc}}/\text{kPa}$	$x_{1,\text{calc}}$	$y_{1,\text{calc}}$		$P_{\text{calc}}/\text{kPa}$	$x_{1,\text{calc}}$	$y_{1,\text{calc}}$	$P_{\text{calc}}/\text{kPa}$	$x_{1,\text{calc}}$	$y_{1,\text{calc}}$
$z_1 = 0.0871$							$z_1 = 0.3620$						
263.15	78.5	0.0668	0.4737	78.5	0.0674	0.4694	288.15	227.7	0.1065	0.4975	227.8	0.1092	0.4971
268.15	93.9	0.0646	0.4467	94.0	0.0653	0.4429	293.15	256.9	0.0982	0.4594	257.0	0.1007	0.4595
273.15	111.7	0.0624	0.4201	111.8	0.0631	0.4169	298.15	289.6	0.0908	0.4229	289.7	0.0931	0.4232
278.15	132.0	0.0602	0.3941	132.1	0.0610	0.3915	303.15	326.3	0.0841	0.3883	326.4	0.0863	0.3888
283.15	155.2	0.0580	0.3688	155.4	0.0588	0.3669	$z_1 = 0.5232$						
288.15	181.5	0.0558	0.3444	181.7	0.0567	0.3430	268.15	274.1	0.3357	0.8539	273.2	0.3392	0.8532
293.15	211.3	0.0537	0.3210	211.5	0.0546	0.3200	273.15	307.3	0.3161	0.8330	306.6	0.3197	0.8325
298.15	244.9	0.0517	0.2986	245.2	0.0525	0.2981	278.15	342.3	0.2969	0.8099	341.7	0.3007	0.8097
303.15	282.7	0.0497	0.2773	282.9	0.0505	0.2772	283.15	379.3	0.2785	0.7847	378.8	0.2824	0.7847
308.15	324.9	0.0477	0.2572	325.2	0.0486	0.2574	288.15	418.4	0.2610	0.7577	418.1	0.2650	0.7579
313.15	372.1	0.0459	0.2382	372.4	0.0468	0.2387	293.15	460.1	0.2446	0.7289	460.0	0.2485	0.7294
318.15	424.7	0.0441	0.2204	424.9	0.0450	0.2211	298.15	504.8	0.2293	0.6988	504.9	0.2331	0.6996
323.15	483.1	0.0425	0.2038	483.2	0.0433	0.2046	303.15	552.8	0.2151	0.6676	553.1	0.2188	0.6687
328.15	547.6	0.0409	0.1882	547.7	0.0417	0.1892	308.15	604.7	0.2020	0.6357	605.1	0.2056	0.6370
333.15	618.9	0.0394	0.1737	618.9	0.0402	0.1748	313.15	660.9	0.1900	0.6034	661.5	0.1935	0.6049
338.15	697.4	0.0380	0.1603	697.3	0.0388	0.1614	318.15	721.9	0.1790	0.5711	722.6	0.1823	0.5728
343.15	783.6	0.0367	0.1478	783.3	0.0374	0.1490	$z_1 = 0.7128$						
348.15	878.1	0.0354	0.1362	877.6	0.0362	0.1374	263.15	262.2	0.4261	0.8954	261.8	0.4300	0.8954
353.15	981.3	0.0342	0.1255	980.6	0.0350	0.1267	268.15	289.6	0.3924	0.8740	289.3	0.3967	0.8740
$z_1 = 0.2980$							273.15	317.7	0.3605	0.8496	317.5	0.3650	0.8498
263.15	172.5	0.2296	0.7936	171.4	0.2317	0.7912	278.15	347.0	0.3309	0.8225	347.0	0.3354	0.8228
268.15	199.5	0.2216	0.7732	198.5	0.2239	0.7710	283.15	378.0	0.3037	0.7928	378.1	0.3083	0.7934
273.15	229.2	0.2135	0.7513	228.2	0.2159	0.7495	288.15	411.1	0.2791	0.7610	411.4	0.2835	0.7618
278.15	261.7	0.2054	0.7282	260.7	0.2079	0.7267	293.15	446.9	0.2569	0.7276	447.2	0.2611	0.7285
283.15	297.1	0.1972	0.7038	296.2	0.1999	0.7027	$z_1 = 0.8015$						
288.15	335.6	0.1892	0.6784	334.9	0.1919	0.6776	268.15	492.4	0.7126	0.9625	491.7	0.7142	0.9628
293.15	377.4	0.1813	0.6520	376.9	0.1841	0.6516	273.15	565.7	0.6958	0.9564	564.9	0.6978	0.9568
298.15	422.9	0.1736	0.6249	422.5	0.1765	0.6248	278.15	643.3	0.6767	0.9490	642.3	0.6792	0.9495
303.15	472.3	0.1662	0.5972	472.1	0.1691	0.5976	283.15	724.2	0.6555	0.9402	723.3	0.6586	0.9408
308.15	526.0	0.1591	0.5692	526.0	0.1620	0.5700	288.15	807.6	0.6324	0.9297	806.9	0.6360	0.9305
313.15	584.4	0.1523	0.5411	584.5	0.1552	0.5422	293.15	892.7	0.6078	0.9174	892.3	0.6120	0.9184
318.15	647.7	0.1459	0.5131	648.1	0.1487	0.5145	298.15	979.1	0.5823	0.9032	979.2	0.5869	0.9044
323.15	716.6	0.1398	0.4854	717.1	0.1426	0.4871	303.15	1066.8	0.5563	0.8870	1067.4	0.5614	0.8885
328.15	791.4	0.1341	0.4581	792.0	0.1368	0.4601	308.15	1155.8	0.5304	0.8689	1157.1	0.5358	0.8706
333.15	872.6	0.1287	0.4315	873.4	0.1314	0.4337	313.15	1246.7	0.5051	0.8489	1248.7	0.5108	0.8509
338.15	960.8	0.1237	0.4056	961.6	0.1262	0.4079	318.15	1340.1	0.4807	0.8271	1342.7	0.4865	0.8294
343.15	1056.4	0.1190	0.3805	1057.3	0.1215	0.3830	$z_1 = 0.8973$						
348.15	1159.9	0.1146	0.3563	1160.9	0.1170	0.3589	268.15	573.8	0.8335	0.9812	573.6	0.8344	0.9815
353.15	1272.0	0.1105	0.3331	1273.0	0.1129	0.3358	273.15	662.6	0.8183	0.9775	662.3	0.8196	0.9778
$z_1 = 0.3620$							278.15	756.7	0.7997	0.9726	756.2	0.8014	0.9731
263.15	123.0	0.1627	0.6931	122.7	0.1659	0.6909	283.15	854.0	0.7773	0.9663	853.5	0.7796	0.9669
268.15	139.6	0.1494	0.6552	139.4	0.1525	0.6534	288.15	952.4	0.7512	0.9583	952.2	0.7541	0.9591
273.15	158.1	0.1371	0.6161	157.9	0.1401	0.6146	293.15	1050.2	0.7216	0.9482	1050.4	0.7253	0.9492
278.15	178.7	0.1259	0.5763	178.6	0.1288	0.5752	298.15	1146.2	0.6896	0.9359	1147.1	0.6940	0.9372
283.15	201.8	0.1157	0.5366	201.8	0.1185	0.5359	303.15	1240.4	0.6563	0.9213	1242.1	0.6613	0.9228

The measured pressures were also compared with values predicted by REFPROP 10.0,<sup>12</sup> which is based on an EoS explicit in reduced Helmholtz energy.<sup>22</sup> Table 4 and Figure 2 provide the deviations between the measured pressures and the values predicted by REFPROP 10.0. Figure 2 clearly shows that REFPROP 10.0 systematically overestimates (deviations from a few percent to well more than  $-20\%$ ) the pressure. The poor agreement likely occurs because the binary interaction parameters contained in REFPROP 10.0 are estimated and not based on experimental data since the publicly available

literature experimental data are absent for the binary pair reported herein. Notwithstanding this fact, comparisons between the experimental data reported herein and REFPROP 10.0 are included because of the widespread use of REFPROP 10.0 in the air conditioning and refrigeration communities. Thus, the large discrepancies should not be taken as an indication of a limitation in REFPROP 10.0 predictions, but rather the predictions are included for completeness and because readers familiar with REFPROP 10.0 would expect such a comparison to be made.

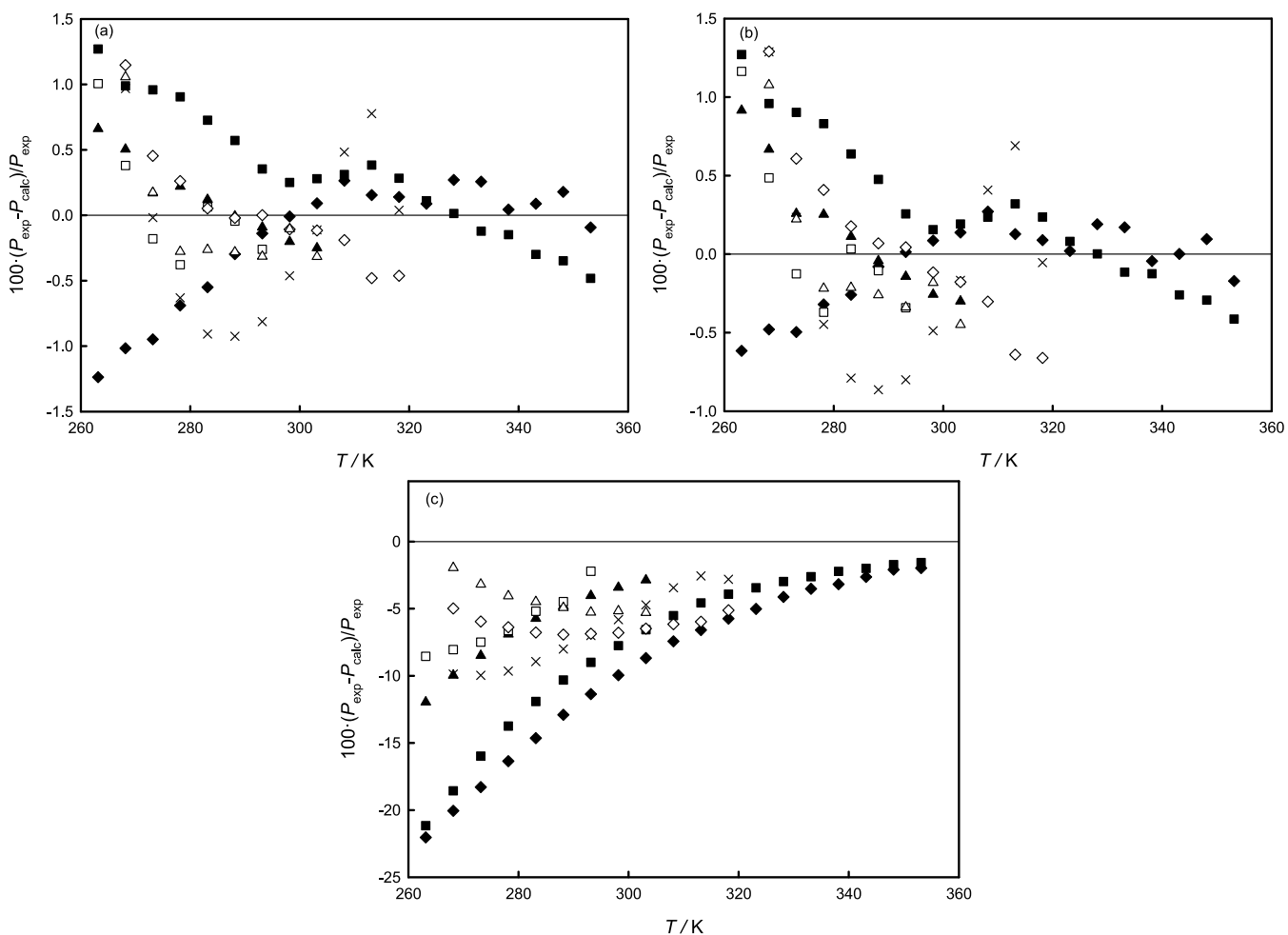


**Figure 2.** Deviations between the measured pressures of the binary blends of R32 (1) + R1234ze(Z) (2) listed in Table SI in the Supporting Information ( $P_{\text{exp}}$ ) and calculated values ( $P_{\text{calc}}$ ) obtained from (a) the “flash method” coupled with the Peng–Robinson EoS using  $k_{12}$  fitted for each isochore, (b) the “flash method” coupled with a cubic EoS proposed by Styjek using  $k_{12}$  fitted for each isochore, and (c) REFPROP 10.0: ■,  $z_1 = 0.0871$  and  $\nu = 0.013352 \text{ m}^3 \cdot \text{kg}^{-1}$ ; ◆,  $z_1 = 0.2980$  and  $\nu = 0.016365 \text{ m}^3 \cdot \text{kg}^{-1}$ ; ▲,  $z_1 = 0.3620$  and  $\nu = 0.071713 \text{ m}^3 \cdot \text{kg}^{-1}$ ; ×,  $z_1 = 0.5232$  and  $\nu = 0.035001 \text{ m}^3 \cdot \text{kg}^{-1}$ ; □,  $z_1 = 0.7128$  and  $\nu = 0.070089 \text{ m}^3 \cdot \text{kg}^{-1}$ ; ◇,  $z_1 = 0.8015$  and  $\nu = 0.023746 \text{ m}^3 \cdot \text{kg}^{-1}$ ; △,  $z_1 = 0.8973$  and  $\nu = 0.026769 \text{ m}^3 \cdot \text{kg}^{-1}$ .

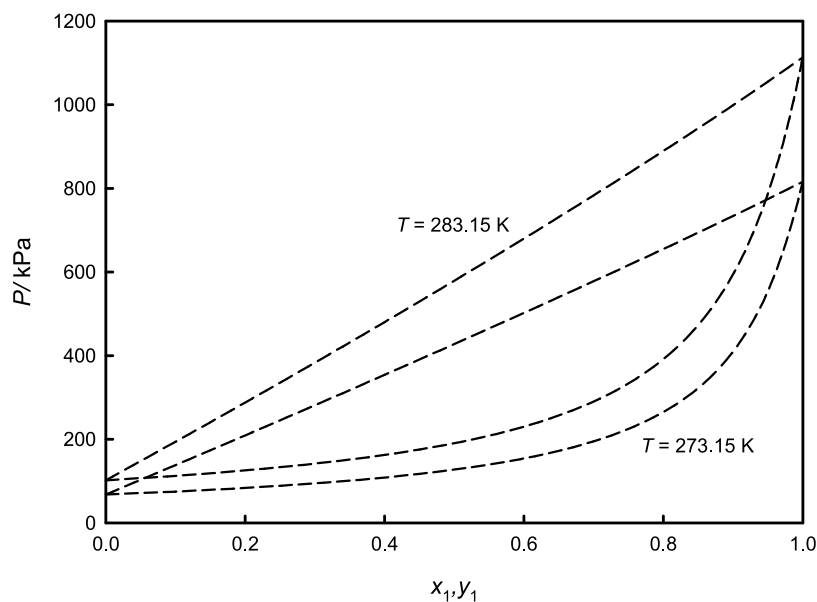


**Figure 3.** VLE representation for the R32 (1) + R1234ze(Z) (2) blends using the Peng–Robinson EoS with  $\bar{k}_{12} = 0.00281$  for  $T = 273.15 \text{ K}$  and  $T = 283.15 \text{ K}$ .

**Table 6.** Coefficients for  $B_{\text{blend}}$  [eq 3] and for  $C_{\text{blend}}$  [eq 4] for R32 (1) + R1234ze(Z) (2) Binary Blends

$B_1$	$B_2$	$B_3$	$B_4$	$B_5$
-1.7750	-923.8710	-98.6313	100.3795	-8.3694
$C_1$	$C_2$	$C_3$	$C_4$	$C_5$
3.6723	1371.0771	104.5247	-70.4911	-29.8528

Figure 3 illustrates the VLE behaviors of the R32 (1) + R1234ze(Z) (2) binary blends calculated at temperatures of 273.15 and 283.15 K using the PR EoS with an average  $k_{12}$  determined by the “flash method”. The resulting value is  $\bar{k}_{1212} = 0.00281$ . Since no experimental data are available in the open literature for blends of R32 + R1234ze(Z), it is not possible to compare the calculated values of Figure 3 with publicly available and experimentally determined VLE properties. It is to be noted that Figure 3 clearly demonstrates ideal behavior per Raoult’s law.

**Correlation of Vapor-Phase  $PvTx$  Properties.** The measured vapor-phase  $PvTx$  data for the R32 (1) + R1234ze(Z) (2) binary blends were correlated with (1) the PR EoS<sup>15</sup> coupled with the van der Waals one-fluid mixing rules,<sup>16</sup> (2) a cubic EoS proposed by Stryjek<sup>17,18</sup> coupled with

the van der Waals one-fluid mixing rules,<sup>16</sup> and (3) a truncated (second order) virial EoS. The measured data were also compared with REFPROP 10.0<sup>12</sup> calculations. The measured vapor-phase data that were located too close to the two-phase region (denoted in Table 3 with a “b”) were excluded during the development of the correlations mentioned above since these data exhibited much higher pressure deviations than data located further from the two-phase region.

Minimizing the AARD ( $P$ ) yielded a  $k_{12}$  value of  $-0.11090$  for the PR EoS<sup>15</sup> coupled with the van der Waals one-fluid mixing rules<sup>16</sup> and a  $k_{12}$  value of  $-0.20463$  for the cubic EoS proposed by Stryjek<sup>17,18</sup> coupled with the van der Waals one-fluid mixing rules.<sup>16</sup> These  $k_{12}$  values yielded AARD ( $P$ ) of 0.49% and 0.53% for the PR EoS<sup>15</sup> and the Stryjek cubic EoS,<sup>17,18</sup> respectively.

As provided in our previous publications,<sup>7–9</sup> the second virial coefficient ( $B_{\text{blend}}$ ) and the third virial coefficient ( $C_{\text{blend}}$ ) employed in the truncated (second order) virial EoS can be fitted to the following functional forms:

$$B_{\text{blend}} = B_1 \ln(T/K) + \frac{B_2}{T} + B_3 x_1^2 + B_4 x_1 + B_5 \quad (3)$$

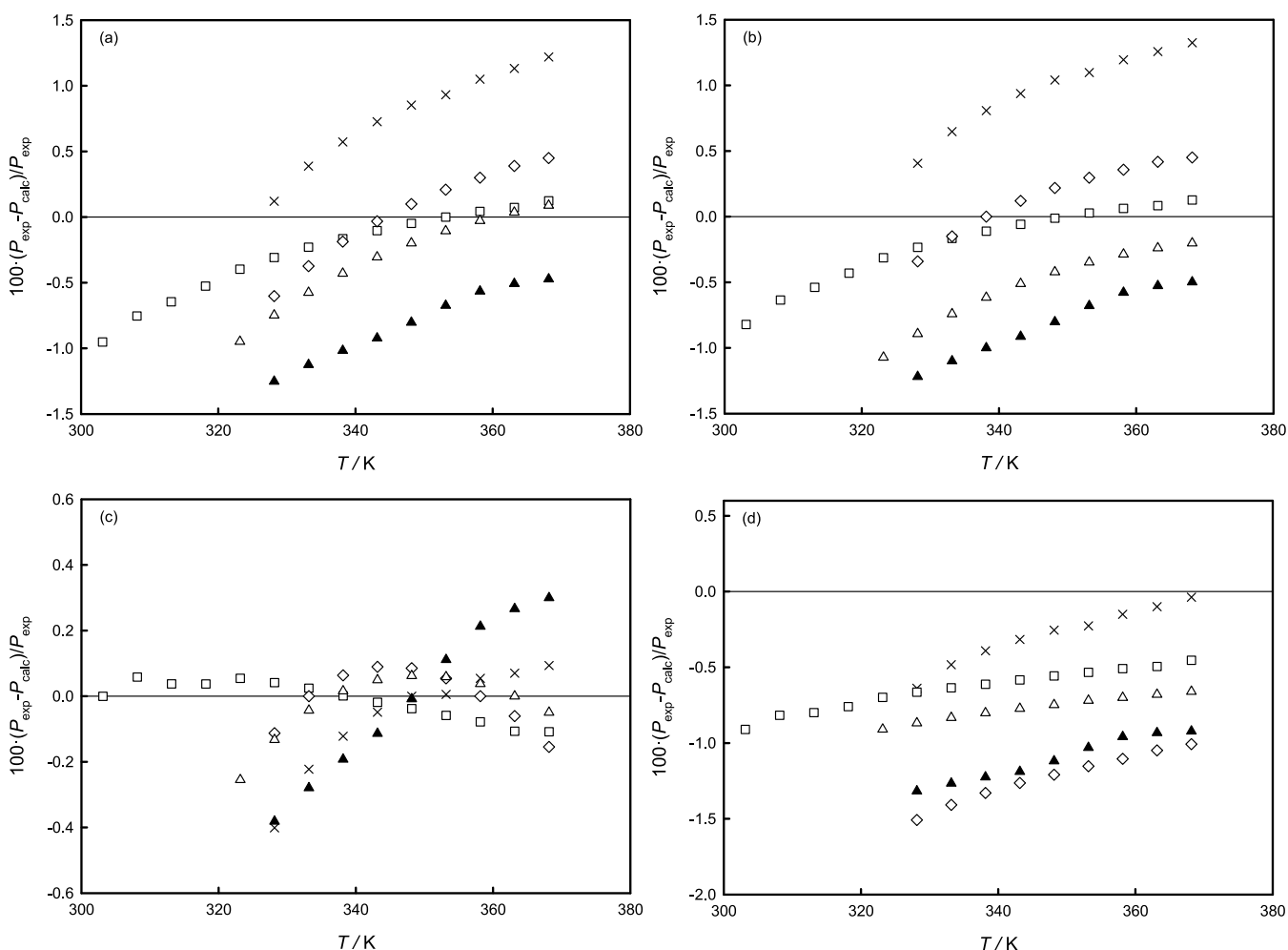


**Figure 4.** Deviations between the measured pressures of the binary blends of R32 (1) + R1234ze(Z) (2) listed in Table 3 ( $P_{\text{exp}}$ ) and calculated values ( $P_{\text{calc}}$ ) determined from (a) the Peng–Robinson EoS, (b) a cubic EoS proposed by Stryjek, (c) the truncated virial EoS, and (d) REFPROP 10.0: ▲,  $z_1 = 0.3620$  and  $\nu = 0.071713 \text{ m}^3 \cdot \text{kg}^{-1}$ ; ×,  $z_1 = 0.5232$  and  $\nu = 0.0355001 \text{ m}^3 \cdot \text{kg}^{-1}$ ; □,  $z_1 = 0.7128$  and  $\nu = 0.070089 \text{ m}^3 \cdot \text{kg}^{-1}$ ; ◇,  $z_1 = 0.8015$  and  $\nu = 0.023746 \text{ m}^3 \cdot \text{kg}^{-1}$ ; △,  $z_1 = 0.8973$  and  $\nu = 0.026769 \text{ m}^3 \cdot \text{kg}^{-1}$ .

$$C_{\text{blend}} = C_1 \ln(T/K) + \frac{C_2}{T} + C_3 x_1^2 + C_4 x_1 + C_5 \quad (4)$$

Table 6 reports the coefficients of eqs 3 and 4, which were determined by minimizing the AARD ( $P$ ) of the vapor phase  $PvTx$  data set. The resulting AARD ( $P$ ) between the vapor-phase  $PvTx$  data of the R32 (1) + R1234ze(Z) (2) binary blends and the values calculated using the truncated (second order) virial EoS is 0.10%.

Finally, the measured  $PvTx$  data were also compared with REFPROP 10.0<sup>12</sup> calculations, yielding an AARD ( $P$ ) = 0.77%.

Figure 4 shows the relative deviations between measured pressure values in the superheated vapor region and (1) the values estimated by the fitting models described above and (2) by REFPROP 10.0.<sup>12</sup> Each of the three fitting models show good agreement with one another and result in small values of AARD ( $P$ ) = 0.77%. It is to be noted, however, that REFPROP 10.0<sup>12</sup> systematically overestimates the pressure predictions.

## CONCLUSIONS

The present paper presents 150  $PvTx$  measurements for binary blends consisting of difluoromethane (R32) and *cis*-1,3,3,3-tetrafluoroprop-1-ene (R1234ze(Z)) both in the two-phase and superheated vapor regions using an isochoric test cell. The superheated vapor data were correlated with the Peng–Robinson (PR) equation of state (EoS), the cubic EoS of Styjek, a truncated (second order) virial EoS, and REFPROP 10.0. The absolute average relative deviation of the pressure (AARD ( $P$ )) for the PR EoS, Styjek EoS, virial EoS, and REFPROP 10.0 were 0.49%, 0.53%, 0.10%, and 0.77%, respectively, indicating good agreement with the measured values. The “flash method” coupled with (1) the PR EoS and the van der Waals one-fluid mixing rules and (2) the Styjek EoS and the van der Waals one-fluid mixing rules were used to derive the VLE data from the two-phase measurements. The AARD ( $P$ ) values for these two methods were 0.38% and 0.37%, respectively. In addition, the VLE data were compared with REFPROP 10.0 predictions, which yielded an unacceptably large AARD ( $P$ ) of 7.12%. This disagreement is not unanticipated since the binary interaction parameters contained in REFPROP 10.0 are estimated and not based on experimental data.

## ASSOCIATED CONTENT

### Supporting Information

The Supporting Information is available free of charge at <https://pubs.acs.org/doi/10.1021/acs.jced.0c00334>.

Values of the  $PvTx$  measurements in the two-phase region (PDF)

## AUTHOR INFORMATION

### Corresponding Author

Giovanni Di Nicola – Dipartimento di Ingegneria Industriale e Scienze Matematiche, Università Politecnica delle Marche, Ancona 60131, Italy; [orcid.org/0000-0001-9582-8764](https://orcid.org/0000-0001-9582-8764); Phone: +39 071 2204277; Email: [g.dinicola@univpm.it](mailto:g.dinicola@univpm.it); Fax: +39 071 2204770

### Authors

Sebastiano Tomassetti – Dipartimento di Ingegneria Industriale e Scienze Matematiche, Università Politecnica delle Marche, Ancona 60131, Italy

Mariano Pierantozzi – Dipartimento di Ingegneria Industriale e Scienze Matematiche, Università Politecnica delle Marche, Ancona 60131, Italy

J. Steven Brown – Department of Mechanical Engineering, The Catholic University of America, Washington, DC 20064, United States; [orcid.org/0000-0003-4914-7778](https://orcid.org/0000-0003-4914-7778)

Complete contact information is available at:

<https://pubs.acs.org/10.1021/acs.jced.0c00334>

### Notes

The authors declare no competing financial interest.

## ACKNOWLEDGMENTS

This work was supported by MIUR of Italy within the framework of the PRIN2015 project “Clean Heating and Cooling Technologies for an Energy Efficient Smart Grid”, Prot. 2015M852PA.

## REFERENCES

- (1) European Parliament, Council of the European Union. Regulation (EU) No 517/2014 of the European Parliament and of the Council of 16 April 2014 on Fluorinated Greenhouse Gases and Repealing Regulation (EC) No 842/2006. *Official J. Eur. Union* **2014**, 195.
- (2) The Kigali Amendment: The Amendment to the Montreal Protocol Agreed by the Twenty-Eighth Meeting of the Parties. *UNEP Ozone Secr.* 2016.
- (3) McLinden, M. O.; Kazakov, A. F.; Steven Brown, J.; Domanski, P. A. A Thermodynamic Analysis of Refrigerants: Possibilities and Tradeoffs for Low-GWP Refrigerants. *Int. J. Refrig.* **2014**, 38, 80–92.
- (4) McLinden, M. O.; Brown, J. S.; Brignoli, R.; Kazakov, A. F.; Domanski, P. A. Limited Options for Low-Global-Warming-Potential Refrigerants. *Nat. Commun.* **2017**, 8, 14476.
- (5) Brown, J. S.; Corvaro, F.; Di Nicola, G.; Giuliani, G.; Pacetti, M. PVT Measurements of Trans-1, 3, 3, 3-Tetrafluoroprop-1-Ene+ Methane and Trans-1, 3, 3, 3-Tetrafluoroprop-1-Ene+ Nitrogen Binary Pairs. *J. Chem. Eng. Data* **2014**, 59 (11), 3798–3804.
- (6) Brown, J. S.; Coccia, G.; Di Nicola, G.; Pierantozzi, M.; Polonara, F. Vapor Phase  $PvTx$  Measurements of Binary Blends of 2, 3, 3, 3-Tetrafluoroprop-1-Ene+ Propane and Cis-1, 2, 3, 3, 3-Pentafluoroprop-1-Ene+ Propane. *J. Chem. Eng. Data* **2016**, 61 (9), 3346–3354.
- (7) Brown, J. S.; Coccia, G.; Tomassetti, S.; Pierantozzi, M.; Di Nicola, G. Vapor Phase  $PvTx$  Measurements of Binary Blends of 2,3,3,3-Tetrafluoroprop-1-Ene + Isobutane and Trans-1,3,3,3-Tetrafluoroprop-1-Ene + Isobutane. *J. Chem. Eng. Data* **2017**, 62 (10), 3577–3584.
- (8) Brown, J. S.; Coccia, G.; Tomassetti, S.; Pierantozzi, M.; Di Nicola, G. Vapor Phase  $PvTx$  Measurements of Binary Blends of Trans-1-Chloro-3,3,3-Trifluoroprop-1-Ene + Isobutane and Cis-1,3,3,3-Tetrafluoroprop-1-Ene + Isobutane. *J. Chem. Eng. Data* **2018**, 63 (1), 169–177.
- (9) Tomassetti, S.; Pierantozzi, M.; Di Nicola, G.; Polonara, F.; Brown, J. S. Vapor-Phase  $PvTx$  Measurements of Binary Blends of Cis-1, 2, 3, 3, 3-Pentafluoroprop-1-Ene+ Isobutane and 3, 3, 3-Trifluoropropene+ Isobutane. *J. Chem. Eng. Data* **2019**, 64, 688.
- (10) Tomassetti, S.; Coccia, G.; Pierantozzi, M.; Di Nicola, G.; Brown, J. S. Vapor Phase and Two-Phase  $PvTx$  Measurements of Difluoromethane+ 2, 3, 3, 3-Tetrafluoroprop-1-Ene. *J. Chem. Thermodyn.* **2020**, 141, 105966.
- (11) Tomassetti, S.; Perera, U. A.; Di Nicola, G.; Pierantozzi, M.; Higashi, Y.; Thu, K. Two-Phase and Vapor-Phase Thermophysical Property ( $PvTx$ ) Measurements of the Difluoromethane + Trans-1,3,3,3-Tetrafluoroprop-1-Ene Binary System. *J. Chem. Eng. Data* **2020**, 65 (4), 1554–1564.
- (12) Lemmon, E. W.; Bell, I. H.; Huber, M. L.; McLinden, M. O. *NIST Standard Reference Database 23: Reference Fluid Thermodynamic*



and Transport Properties-REFPROP, version 10.0; National Institute of Standards and Technology: 2018, <http://www.nist.gov/srd/nist23.cfm>.

(13) Giuliani, G.; Kumar, S.; Polonara, F. A Constant Volume Apparatus for Vapour Pressure and Gas Phase P-V-T Measurements: Validation with Data for R22 and R134a. *Fluid Phase Equilib.* **1995**, *109* (2), 265–279.

(14) Di Nicola, G.; Polonara, F.; Ricci, R.; Stryjek, R. PVTx Measurements for the R116+ CO<sub>2</sub> and R41+ CO<sub>2</sub> Systems. New Isochoric Apparatus. *J. Chem. Eng. Data* **2005**, *50* (2), 312–318.

(15) Peng, D.-Y.; Robinson, D. B. A New Two-Constant Equation of State. *Ind. Eng. Chem. Fundam.* **1976**, *15* (1), 59.

(16) Poling, B. E.; Prausnitz, J. M.; O'Connell, J. P. *The Properties of Gases and Liquids*, 5th ed.; McGraw-Hill, 2001.

(17) Stryjek, R. Correlation and Critical-Evaluation of Vle Data for Nitrogen+ Argon, Nitrogen+ Methane, and Argon+ Methane Mixtures. *Bull. Polish Acad. Sci.* **1991**, *39* (4), 353–361.

(18) Stryjek, R. On the Prediction of the Gas-Liquid Critical Locus with Cubic Equations of State. *Bull. Polish Acad. Sci.* **1992**, *40* (3), 211–220.

(19) Di Nicola, G.; Coccia, G.; Pierantozzi, M.; Tomassetti, S. Vapor-Liquid Equilibrium of Binary Systems Containing Low GWP Refrigerants with Cubic Equations of State. *Energy Procedia* **2018**, *148*, 1246–1253.

(20) Di Nicola, G.; Coccia, G.; Pierantozzi, M.; Tomassetti, S.; Stryjek, R. Analysis of Vapor Pressure and VLE of HFOS, HCFOS, and Their Blends with Cubic Equations of State. In *Refrigeration Science and Technology*; International Institute of Refrigeration: 2018; Part F1476, pp 403–412, DOI: 10.18462/iir.hfo.2018.1166.

(21) Di Nicola, G.; Giuliani, G.; Passerini, G.; Polonara, F.; Stryjek, R. Vapor-Liquid-Equilibrium (VLE) Properties of R-32 + R-134a System Derived from Isochoric Measurements. *Fluid Phase Equilib.* **1998**, *153* (1), 143–165.

(22) Bell, I. H.; Lemmon, E. W. Automatic Fitting of Binary Interaction Parameters for Multi-Fluid Helmholtz-Energy-Explicit Mixture Models. *J. Chem. Eng. Data* **2016**, *61* (11), 3752–3760.